Proc. Natl. Acad. Sci. USA
Vol. 75, No. 9, pp. 4165–4169, September 1978
Biochemistry

Kinetic factors and form determination of the head of bacteriophage T4

(protein–protein interactions/length determination/assembly/electron microscopy/evolution)

MICHAEL K. SHOWE AND LOUISE ONORATO

Department of Microbiology, Biozentrum of the University of Basel, Klingelbergstrasse 70, CH-4056 Basel, Switzerland

Communicated by William B. Wood, June 5, 1978

ABSTRACT **The form of the bacteriophage T4 prehead is described by its icosahedral symmetry, its diameter, and its length. We show how each of these parameters is regulated during prehead formation and ascribe specific form-determining functions to the prehead proteins. The major protein of the head shell can assemble in several different forms. The structure produced *in vivo* depends on the rate of synthesis of the major protein relative to the rates of synthesis of minor shell proteins and the major core protein. From our observations, we propose a model for form determination of the prehead and suggest a pathway for the evolution of its prolate shape.**

The head of bacteriophage T4 has been extensively studied as a model for discovering mechanisms of form determination of biological structures. It is a prolate icosahedron of triangulation number (T) = 13 (1, 2) elongated on its 5-fold axis of symmetry (3), with a length-to-width ratio of 1.37 (4). It is assembled on the *Escherichia coli* inner membrane as a core-containing prehead (5), which is matured to the finished head by a series of reactions that includes limited proteolysis of capsid and core proteins, expansion of the prehead shell lattice, and packaging of the phage DNA (6). The relatively large size and the prolate shape of the T4 head suggest that the prehead [in which the form is already determined (4)] cannot be produced by simple self-assembly of the shell protein, as is possible with small regular icosahedral viruses (7, 8).

A number of mechanisms have been proposed (9, 10) to account for form determination in the assembly of large or anisometric virus shells or other structures in which simple self-assembly of identical subunits is not possible (11). They include regulation by a genetically defined "measuring rod" or template, a vernier, and accumulating strain with the addition of subunits. Of these, only the "measuring rod" model, (the determination of the length of tobacco mosaic virus by its RNA) has been experimentally demonstrated (12, 13). All of these models depend strongly on specific interactions between the polymerizing subunits, but Wagenknecht and Bloomfield (14) have shown theoretically how the length of linear aggregates might also depend on the concentration of the polymerizing subunits.

Recent observations on the role of minor proteins in prehead formation, and on changes in prehead length that depend on subunit concentrations, suggest that kinetic factors as well as specific protein–protein interactions regulate the form of the T4 prehead.

The form of the T4 prehead is described by its symmetry (icosahedral), its width, and its length (extension along the 5-fold axis of symmetry). We account for these in the following way. The symmetry is determined by formation of a 5-fold symmetric initiation complex that directs assembly of the shell into closed structures instead of open tubes. The width is determined by the intrinsic curvature of the shell and the diameter of the core that it must enclose. The length can be varied. It is regulated by the relative rates of growth of the core and the shell from the initiation complex, and also by the rate of induction or stabilization of the distal vertices of the icosahedral shell.

Form-determining components of the T4 prehead-symmetry determination

Fig. 1 shows the structure and protein composition of the normal T4 prehead and the mature head. The core, as well as the shell, of the prehead is attached to the bacterial membrane (5) by an apparent icosahedral vertex (Fig. 2). The membrane attachment vertex (or proximal vertex) is probably also the tail attachment site, because its structure is different from that of the other vertices (18).

The form of the T4 prehead is determined by the products of the "head genes," which are sequentially clustered on the genetic map in the order *20, PIP, 21, 22, 23, 24* (Table 1). Other prehead components are nonessential for prehead production, and their genes map outside this cluster. The products of two other known genes, [*31*, whose mutants yield only precipitates of the major head protein (27, 28), and *40*, whose mutants make polyheads (27)], are required for normal prehead formation. Their functions are unknown, but neither of them is a prehead component (21). At least 10 other genes are required to produce a mature head, but mutants in these produce morphologically normal structures that are blocked at late steps in head maturation (16).

Of the proteins listed in Table 1, least is known about PIP (precursor to internal peptide). It is a core component that is cleaved to trichloroacetic acid-soluble fragments by the T4 maturation protease (T4PPase) (20). No mutant has been isolated with a lesion in this gene. P21† is the precursor to T4 prehead proteinase. It seems to have no morphopoietic function because all mutants in this gene produce morphologically normal preheads that are only blocked in maturation (22, 29, 30). P21 is not found in 20^- polyheads (our unpublished observation), suggesting that it is associated with one or more of the vertices of the prehead core.

Mutants in gene *20* make open-ended tubular polyheads with cores composed of P22 and the internal proteins (31) and PIP (our unpublished observation). Like all polyheads, their shells are composed of hexamers of the major capsid protein, P23, arranged in a hexagonal lattice that may have various foldings (pitch angles and diameters) but never the (u, v = 5, 15) folding characteristic of preheads (36). Because polyheads have open ends, it was suggested (29) that P20 is essential for cap formation. By chemical extraction of capsids, we showed that P20 is not present at the 11 nonproximal vertices, but is removed with

The publication costs of this article were defrayed in part by page charge payment. This article must therefore be hereby marked "*advertisement*" in accordance with 18 U. S. C. §1734 solely to indicate this fact.

† The protein products of numbered genes are abbreviated P followed by the gene number. An asterisk denotes a cleaved gene product. Mutants are described by gene number followed by the site in parentheses.

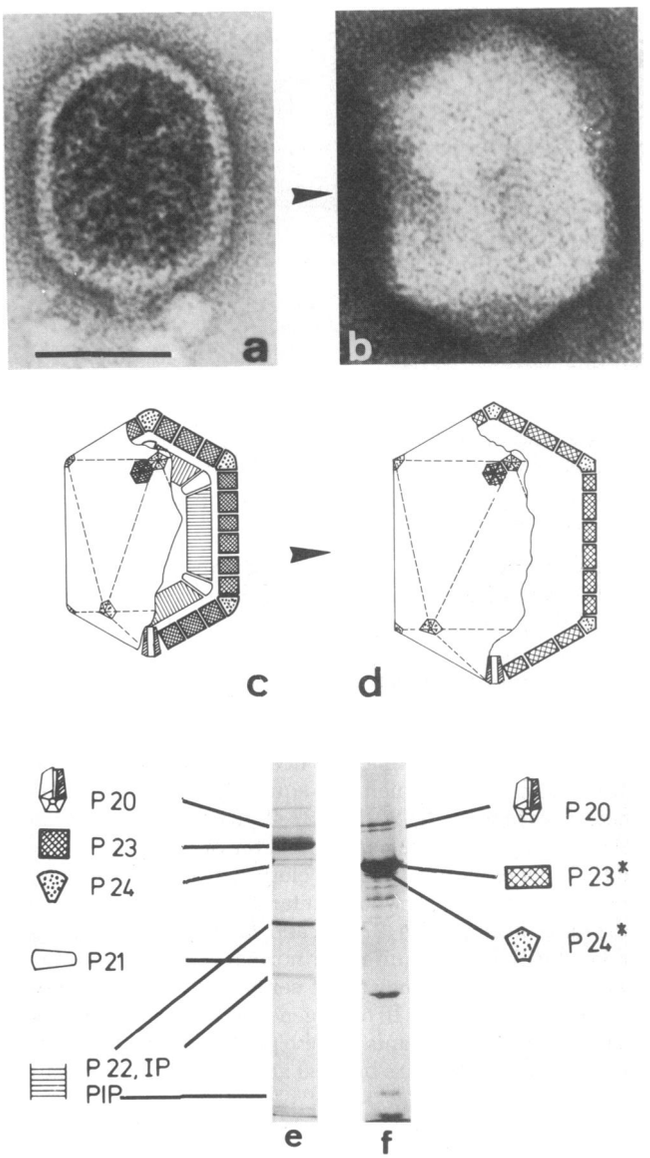

FIG. 1. Structure and composition of the T4 prehead and mature head. (*a*) Prehead of a mutant in gene *21* (tsN8). The bar represents 50 nm. (*b*) Mature head from a tail$^-$ mutant, *10* (amB255)–*18* (amE18). (*c*) Model for the prehead based on the text. P21 is placed at the core vertices because its activity is controlled by P24, and it is present in about 60 copies per prehead (15). The core is shown as an icosahedron, but this structure is not established. (*d*) Model for the mature head. The DNA is omitted from the diagram. (*e*) Acrylamide (12.5%)/sodium dodecyl sulfate gel of *21* (ts N8) preheads purified by glycerol gradient centrifugation. (*f*) Acrylamide (12.5%)/sodium dodecyl sulfate gel of mature heads purified as for *e*. Sodium dodecyl sulfate gels and sample preparation for them have been described (15). Electron microscopy is described under Fig. 2.

a structure at the tail attachment site (18). We proposed that it initiates prehead formation at this site by establishing a 5-fold axis of symmetry that permits formation of structures that, because of their lattice folding, are able to form caps (15, 17).

The remaining genes—*22*, *23*, and *24*—code for, respectively, the principal component of the prehead core, the major protein of the prehead shell, and the vertex protein. The length and width of the prehead are determined by the aggregation properties and concentrations of these gene products in the infected cells, as discussed below.

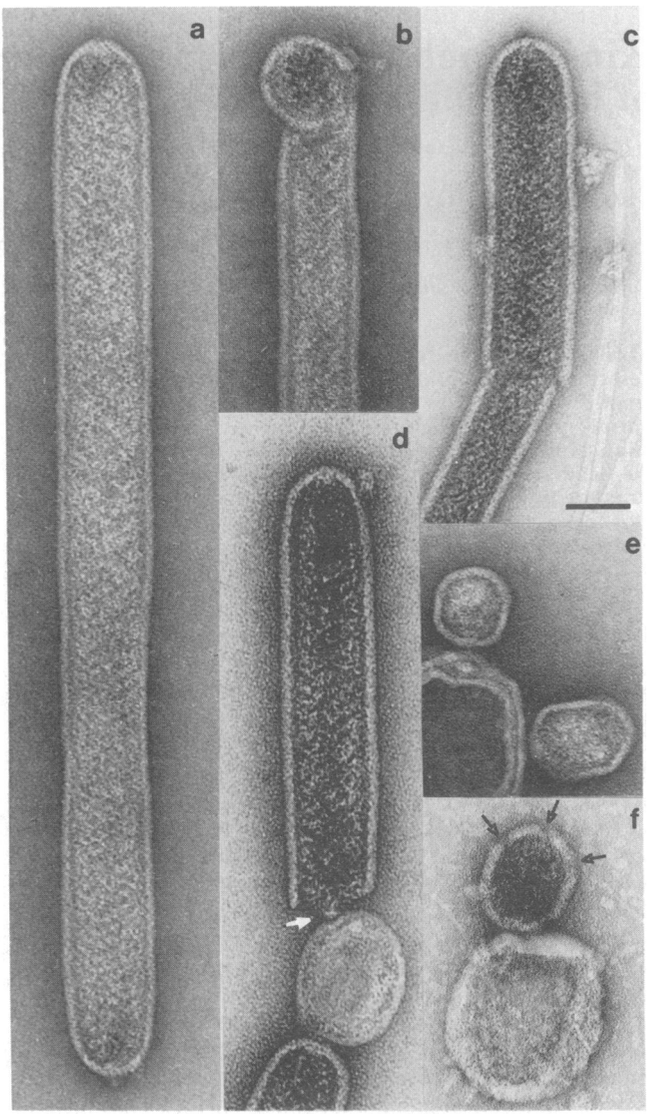

FIG. 2. Preheads and polyheads from *24* (amN65) lysates. Microscopy was carried out as described previously (15) except that 2% uranyl acetate was used as the negative stain. Micrographs were recorded on a Philips 300 electron microscope operating at 80 kV at a magnification of ×45,000. The bar represents 50 nm. (*a*) Giant prehead. (*b*) Prehead growing a polyhead from nonproximal vertices. (*c*) Giant prehead growing a polyhead (note the decreased diameter of shell and core of the polyhead. (*d*) Two giant preheads attached to a membrane vesicle. The arrow shows the core attached to the vesicle where the cap was broken away. (*e*) An isometric and a normal prehead after addition of P24 to complete the vertices. (*f*) A prehead on a vesicle shown before P24 addition. The arrows show the gaps at the vertex positions.

Determination of the length and width of the prehead

Amber mutants and temperature-sensitive mutants in gene 22 produce multilayered open-ended polyheads with no or unstable cores (29, 31). The production of polyheads instead of preheads by 22$^-$ mutants suggests that P22 acts with P20 and P40 in prehead initiation. P22 is the major core component of preheads (32) and polyheads (31). In its absence, polyheads are produced with a surface lattice line of higher curvature than those of core-containing polyheads or preheads (17). Thus, normal cores appear to limit the curvature that the P23 shell can attain; preheads are wider than 20$^-$ polyheads and their cores are also about 40% wider (25).

Two temperature-sensitive mutants in gene *22* produce, at semipermissive temperatures, both normal and petite phage

Table 1. Characteristics of some prehead proteins

Gene	Protein molecular weight (ref.)	Isoelectric point in 6 M urea	Structures produced by mutants	Function	Copies per prehead (15)	Cleavage products after head maturation
20	65,000 (19)	—	Polyheads with open ends and stable cores	Prehead initiation, establish membrane attachment	15	Not cleaved
PIP	13,000 (20)	4.8	No mutants isolated	Core of preheads and polyheads	200	Peptides, one remains in head
21	26,000 (21) 27,500 (22)	5.6	Prehead blocked in cleavage reactions	Precursor to T4 protease	50	Peptides
22	27,500 (23) 32,000 (32)	5.3	Open-ended, multilayered polyheads,* petite phage with mainly regular icosahedral heads†	Major core protein guides shell assembly of prehead	500–600	Peptides, one remains in head
23	55,000 (19) 58,300 (23)	6.2	No head-shell structures, ‡ highly deformed preheads§	Major prehead protein, polyhead shell protein	1000	Major head protein, molecular weight 47,700 (23)
24	47,000 (19) 48,400 (23)	5.5	Preheads and elongated preheads with gaps at vertex positions,* giant phages†	Vertex protein of prehead	60	Head vertex protein, molecular weight 45,000 (19)

Isoelectric points were determined by focusing in 6 M urea on thin layers of Sephadex G-75 superfine of *20* (amB8)–*21* (N90) polyheads and *21* (tsN8) preheads dissociated in 1 mM potassium phosphate buffer, pH 6–7 (34). The isolation of polyheads has been described (24). The preheads were isolated by differential centrifugation by a similar procedure; details will be described elsewhere (15). References not listed in the table for gene product properties are cited in the text.

* Amber (am) or temperature-sensitive (ts) mutant grown at nonpermissive condition.

† Temperature-sensitive mutant grown at semipermissive condition.

‡ Amber mutant grown on nonpermissive host.

§ Temperature-sensitive mutant grown at nonpermissive temperature.

(33). The latter have isometric or slightly elongated heads of normal width. The percentage of these petites increases with temperature to 86%. The finding that two different mutants have the same phenotype argues against a specific shape-determining alteration in core–shell interactions. We suggest that the increase in temperature decreases the effective concentration of active P22 in the cell, and that the rate of core growth is thereby decreased. The inherent curvature of the P23 shell then results in the formation of short preheads because the growth of the core lags behind that of the shell.

P23 is the shell protein of preheads and polyheads (27). The hexagonal P23 lattice must have inherent curvature, because purified P23 assembles into polyheads (34). Polyheads assembled *in vivo* with cores have a near-equatorial lattice line with the same radius of curvature as preheads (17). We propose, on the basis of these findings, that the diameter of the prehead is uniquely specified by its initiation at a P20-containing structure with 5-fold symmetry and the growth of a shell having one lattice line with the maximum curvature consistent with the width of the prehead core. On this model, narrower preheads with the 10, 5 lattice folding characteristic of some polyheads cannot be formed because the prehead core initiated by P20 is too wide.

Five missense mutants in gene *23* have been described (4, 35). Of these, two (the pt mutants) produce normal and petite phage, and three (the ptg mutants) produce phage with petite, normal, and also "giant" heads. The latter have the normal head width but their head length varies between 1.5 and 8 times that of wild-type T4 (35). It has been suggested (25) that the petite producer (ptE920g) synthesizes P23 with either a higher than normal intrinsic curvature or with a lower affinity for the core. We shall argue below that the petite phenotype results from the ability of the mutated P23 to induce precocious closing of the prehead by substituting for P24 at the vertices of the distal cap. The ptg phenotype is probably also based on an alteration in vertex stabilization.

Amber and temperature-sensitive mutations in gene *24* have been described as giving rise to τ particles [since shown to be nearly normal preheads (26)] and polyheads (29). Temperature-sensitive mutants in gene *24*, grown at intermediate temperatures, produce small numbers of infectious giant phage (36). P24 forms the nonproximal vertices of the prehead, and P24* those of the mature capsid (15). The membrane-bound 24^- preheads (Fig. 2) have gaps at their nonproximal vertices. The addition of P24 stabilizes the preheads by filling these gaps, and the preheads then cleave and mature to capsids (15). *In vivo*, then, P24 addition probably terminates prehead assembly and initiates maturation.

Of the "polyheads" found in fresh lysates of 24^- mutants, we find a high percentage are normally closed at one or both ends and possess the 5, 15 lattice folding characteristic of giant preheads. Of the remainder, many, if not all, appear to arise from a normal or a giant prehead by a change in lattice folding during growth of the particle (Fig. 2). We infer that the polyheads produced by 24^- mutants are all initiated as preheads with the proper 5, 15 lattice folding. Giant phages arise from maturation of the few properly completed giant preheads.

Taken together, these results show that P24 functions late in normal prehead assembly, after core and shell growth are complete, to close the pentameric vertices and trigger the maturation cleavages. When P24 is deficient, the distal cap appears to be unstable and subject to dissociation, with the result that the prehead formed may be short, normal, or extra-long, or it may continue to grow around a partially closed particle.

Alteration in T4 head length by gene dosage

The effect on T4 prehead length of various concentrations of the stoichiometrically required (37) prehead proteins can be directly tested by simultaneous mixed infections using wild-type and amber mutants (Table 2). Reduction in the amount of P24 by coinfecting cells with a mixture of wild-type and *24*$^-$ amber mutant (line 1) results in the formation of both petite and giant phages, in agreement with a requirement for P24 to stabilize prehead vertices. Reduction in the synthesis of P23 leads to an increase in the formation of elongated particles and a decrease in the formation of petites (lines 2, 3), while a decrease in P22 has the opposite effect (lines 4, 5). The effects cancel when P22 and P23 are simultaneously reduced (line 6). These results agree with our suggestion that competition between core and shell synthesis regulates prehead length.

The effect of P23 levels on particle length is also shown in lines 7–12 of Table 2. The percent of petite particles produced by mixed infection of *23* (ptE920g) with an amber mutant in gene *23* can be reduced to zero, while the mixed infection with wild type causes a much lower reduction. This demonstrates that the length of the particles produced depends on the ratio of P23 to the other head gene products, because the presence of additional *normal* P23 in the mutant-infected cell results in a *higher* percentage of petite phage than the presence of the mutant protein alone.

The missense mutant in gene *23* called "bypass 24" (byp 24) produces viable phage without P24 (39), i.e., when combined in the double mutant *23* (byp 24)–*24* (am). byp 24 is temperature sensitive, producing fewer particles, of which an increasing percentage are petite, as the growth temperature is raised from 30° to 42°. The double mutant is cold sensitive, producing viable phage (with normal length heads) only above 30°. We have found that the petite producer *23* (ptE920g) has identical properties. It is also a bypass 24, even though the mutation maps (35) at the opposite end of gene *23*. Because it had been suggested (39) that the bypass phenotype might result from the substitution of the byp P23 for P24, we tested the effect of the reduction of P24 levels on head size of the petite mutant. As the P24 is reduced, the percent of petite phage is reduced (Table 2, lines 13–16), showing that the pt phenotype results from an overproduction of P24 activity. We propose that, at higher temperatures, the mutant P23 is increasingly able to substitute for P24 at the prehead vertices, and that this "excess P24" induces precocious closing of the prehead. When no P24 is present (as in the double mutant), the mutant P23 has enough vertex-forming activity to complete normal preheads at high temperature, but there is not sufficient excess to induce the formation of petites.

Kinetic effects and specific interactions in form determination

We propose that the width of the prehead is an expression of the intrinsic curvature of the hexagonal P23 lattice (limited by the core) and therefore is a function of specific P23–P23 bonding. This property suggests that P23 might self-assemble with core components into preheads. Because preheads are formed from a lower level of precursors than polyheads (40), they might appear to be the energetically favored end-product of precursor aggregation. We suggest there is a kinetic limitation to the self-assembly of such an icosahedral, doubly curved structure. In the absence of an initiator with 5-fold symmetry, which requires P20, and probably P22, five P23 hexamers would have to align themselves properly around a pentameric "hole." Instead, in the absence of the initiator, there is an energetic compromise between the curvature intrinsic to the P23–P23 bonding and the resistance of a hexagonal lattice to curve in more than one direction. The result is a tube, or polyhead, which satisfies the intrinsic curvature of P23 in one direction and the geometrical requirements of a hexagonal lattice in the other.

We have shown that the length of the T4 preheads made *in vivo* can be altered by varying the relative levels of the major core protein, the shell protein, and the vertex protein. The extremely low levels of petite or giant phage found on infection with T4 wild type reflects the specifically balanced rates of transcription and translation of these proteins. When this balance is altered experimentally to produce shorter preheads, the resulting population contains mainly petite and/or normal

Table 2. Alterations in T4 head length by mixed infection

	Mutant 1		Mutant 2			
	Mutant	moi	Mutant	moi	% giants	% petites
1	*24* (amC31)	5	T4$^+$	5	0.015	4
2	*24* (amC31)	5	*23* (amE506)	5	0.047	0
3	*24* (amC31)	5	*23* (amB17)	5	0.053	0.5
4	T4$^+$	15	—	0	0	0.29
5	T4$^+$	7.5	*22* (amE209)	7.5	0	7.3
6	T4$^+$	7.5	*22* (amE209)–*23* (amB17)	7.5	0	0.19
7	*23* (ptE920g)	17	T4$^+$	3	–	48
8	*23* (ptE920g)	10	T4$^+$	10	–	31
9	*23* (ptE920g)	3	T4$^+$	17	–	18
10	*23* (ptE920g)	17	*23* (amB17)	3	–	30
11	*23* (ptE920g)	10	*23* (amB17)	10	–	6
12	*23* (ptE920g)	3	*23* (amB17)	17	–	0
13	*23* (ptE920g)	15	*23* (ptE920g)–*24* (amN65)	0	0	60
14	*23* (ptE920g)	10	*23* (ptE920g)–*24* (amN65)	5	0	20
15	*23* (ptE920g)	5	*23* (ptE920g)–*24* (amN65)	10	0	2
16	*23* (ptE920g)	0	*23* (ptE920g)–*24* (amN65)	15	0	0

moi, multiplicity of infection. Data in lines 1–3 are from ref. 38; data in lines 7–12 are from ref. 4. Data from our own experiments (lines 4–6 and 13–16) were obtained from lysis-inhibited cultures grown for 60 min at 37°. Cultures were concentrated 50-fold by centrifugation and lysed with chloroform, and phage in the lysate were counted directly in the microscope after staining with 1% uranyl acetate.

heads and about 10% of intermediate lengths (ref. 39 and our observations). The presence of these intermediate heads is consistent with our model for prehead closing controlled by core growth and vertex induction. However, the predominance of two size classes suggests that core growth may slow or pause at specific lengths determined by its own structure. The recent demonstration (41) that core proteins can assemble *in vitro* with P20 to give core-like aggregates of limited, rather than indefinite, length argues that specific interactions among the core proteins also influence the length of the prehead that is formed.

Evolutionary considerations

Architectural simplicity suggests that a T4 with a regular icosahedral head was a probable evolutionary precursor to the modern T4 phage. About one-third of the modern T4 genome can be deleted without the loss of any essential function (42). Such a reduced genome could be packed into a petite phage head (4). We propose that the prolate head of modern T4 evolved to allow the incorporation of the additional genes now found on the chromosome. The properties of products of the T4 head genes *PIP* through *24* listed in Table 1 suggest a possible mechanism for such a development. The molecular weights of these proteins are all near multiples of the lowest, 13,000, and increase regularly with their order on the genetic map. The core proteins P21 and P22 appear to have arisen by successive duplications and fusion of a precursor protein the size of *PIP*, and the shell proteins from these by the same process. These relationships are supported by other properties listed in Table I, and by the amino acid compositions of those proteins that have been isolated (23). We have already suggested (30) that the protease evolved from a duplication of gene 22. Coliphage P22 is matured without limited proteolysis (43), and because it also lacks the sophisticated tail of T4, it may be considered a more primitive phage, lacking both a protease and a contractile tail.

The petite mutant, in which P24 is dispensable, provides a clue to the evolution of the prolate head shape. We suggest that a primitive form of T4, having only a duplication of a precursor to gene 23 (instead of 23 and 24) produced petite phage. An increase in the efficiency of transcription or translation of the core protein then introduced the possibility of the production of prolate heads with an increased DNA-packaging capability. The selective advantage of this capability then led to the divergence of P23 and P24 to separate hexamer-forming and pentamer forming subunits.

We gratefully acknowledge helpful discussions with Drs. Edward Kellenberger, Ueli Aebi, and Roel van Driel, and we thank Dr. van Driel for his critical reading of the manuscript and Dr. M. Wurtz for drawing the diagrams of Fig. 1. This work was supported by grant AI-13165 from the National Institutes of Health and a National Institutes of Health postdoctoral fellowship to L.O.

1. Branton, D. & Klug, A. (1975) *J. Mol. Biol.* **92,** 559–565.
2. Aebi, U., Bijlenga, R. K. L., van den Broek, J., van den Broek, R., Eiserling, F., Kellenberger, C., Kellenberger, E., Mesyanzhinov, V., Müller, L., Showe, M. K., Smith, R. & Steven, A. (1975) *J. Supramol. Struct.* **2,** 253–275.
3. Moody, M. F. (1965) *Virology* **26,** 567–576.
4. Eiserling, F. A., Geiduschek, E. P., Epstein, R. H. & Metter, E. J. (1970) *J. Virology* **6,** 865–876.
5. Simon, L. D. (1972) *Proc. Natl. Acad. Sci. USA* **69,** 907–911.
6. Showe, M. K. & Kellenberger, E. (1975) in *Control Processes in Virus Multiplication*, eds., Burke, D. C. & Russell, W. C. (Cambridge University Press, Cambridge), pp. 407–438.
7. Bancroft, J. B. (1970) *Adv. Virus Res.* **16,** 99–133.
8. Knolle, P. & Hohn, T. (1975) *RNA Phages*, ed. Zinder, N. D. (Cold Spring Harbor Laboratory, Cold Spring Harbor, NY, pp. 147–201.
9. Kellenberger, E. (1969) in *Symmetry and Function of Biological Systems at the Macromolecular Level*, eds. Engstrom, A. & Stranberg, B. (Alquist and Wicksell, Stockholm, Sweden), pp. 349–366.
10. Kellenberger, E. (1972) *Polymerization in Biological Systems*, Ciba Foundation Symposia No. 7, eds. Wolstenholme, G. E. & O'Connor, M. (Associated Scientific Publishers, Amsterdam, Netherlands), pp. 295–298.
11. Caspar, D. L. D. & Klug, A. (1962) *Cold Spring Harbor Symp. Quant. Biol.* **27,** 1–24.
12. Lebeurier, G., Nicolaieff, A. & Richards, K. E. (1977) *Proc. Natl. Acad. Sci. USA* **74,** 149–153.
13. Otsuki, Y., Takebe, I., Ohno, T., Fukuda, M. & Okada, Y. (1977) *Proc. Natl. Acad. Sci. USA* **74,** 1913–1917.
14. Wagenknecht, T. & Bloomfield, V. (1975) *Biopolymers* **14,** 2297–2309.
15. Onorato, L., Stirmer, B. & Showe, M. K. (1978) *J. Virol.* **27,** 409–426.
16. Wood, W. B., Edgar, R. S., King, J., Lielausis, I. & Henninger, M. (1968) *Fed. Proc. Fed. Am. Soc. Exp. Biol.* **27,** 1160–1166.
17. Steven, A. C., Aebi, U. & Showe, M. K. (1976) *J. Mol. Biol.* **102,** 373–407.
18. Müller-Salamin, L., Onorato, L. & Showe, M. K. (1977) *J. Virology* **24,** 121–134.
19. Vanderslice, R. & Yegian, C. D. (1974) *Virology* **60,** 265–275.
20. Kurtz, M. & Champe, S. (1977) *J. Virol.* **22,** 412–419.
21. Castillo, C. J., Hsiao, C. L., Coon, P. & Black, L. W. (1977) *J. Mol. Biol.* **110,** 585–602.
22. Showe, M. K., Isobe, E. & Onorato, L. (1976) *J. Mol. Biol.* **107,** 55–69.
23. Tsugita, A., Black, L. W. & Showe, M. K. (1975) *J. Mol. Biol.* **98,** 271–275.
24. Steven, A. C., Couture, E., Aebi, U. & Showe, M. K. (1976) *J. Mol. Biol.* **106,** 187–221.
25. Paulson, J. R. & Laemmli, U. (1977) *J. Mol. Biol.* **111,** 459–485.
26. Bijlenga, R. K. L., van den Broek, R. & Kellenberger, E. (1974) *Nature (London)* **249,** 825–827.
27. Epstein, R. H., Bolle, A., Steinberg, C. M., Kellenberger, E., Boy de la Tour, E., Chevalley, R., Edgar, R. S., Susman, M., Denhardt, G. H. & Lielausis, A. (1963) *Cold Spring Harbor Symp. Quant. Biol.* **28,** 375–394.
28. Laemmli, U. K., Béguin, F. & Gujer-Kellenberger, G. (1970) *J. Mol. Biol.* **47,** 69–85.
29. Laemmli, U. K., Mölbert, E., Showe, M. & Kellenberger, E. (1970) *J. Mol. Biol.* **49,** 99–113.
30. Showe, M. K., Isobe, E. & Onorato, L. (1976) *J. Mol. Biol.* **107,** 35–54.
31. Laemmli, U. K. & Quittner, S. F. (1974) *Virology* **62,** 483–499.
32. Showe, M. K. & Black, L. W. (1973) *Nature (London)* **242,** 70–75.
33. Paulson, J. R., Lazaroff, S. & Laemmli, U. K. (1976) *J. Mol. Biol.* **103,** 155–174.
34. van Driel, R. (1977) *J. Mol. Biol.* **114,** 61–72.
35. Doermann, A. H., Eiserling, F. A. & Boehner, L. (1973) *Virus Research*, eds. Fox, C. F. & Robinson, W. S. (Academic, New York), pp. 243–257.
36. Bijlenga, R. K. L., Aebi, U. & Kellenberger, E. (1976) *J. Mol. Biol.* **103,** 469–498.
37. Snustad, P. D. (1968) *Virology* **35,** 550–568.
38. Cummings, D. J. & Bolin, R. W. (1975) *Bacteriol. Rev.* **40,** 314–359.
39. McNicol, L. A., Simon, L. D. & Black, L. W. (1977) *J. Mol. Biol.* **116,** 261–283.
40. Laemmli, U. K. & Eiserling, F. A. (1968) *Mol. Gen. Genet.* **101,** 333–345.
41. van Driel, R. & Couture, E. *J. Mol. Biol.*, in press.
42. Wood, W. B. & Revel, H. R. (1976) *Bacteriol. Rev.* **40,** 847–868.
43. King, J. & Casjens, S. R. (1974) *Nature (London)* **251,** 112–119.